

## IRON $K\alpha$ EMISSION FROM X-RAY REFLECTION: PREDICTIONS FOR GAMMA-RAY BURST MODELS

DAVID R. BALLANTYNE AND ENRICO RAMIREZ-RUIZ

Institute of Astronomy, University of Cambridge, Madingley Road, Cambridge CB3 0HA, England, UK

Received 2001 June 11; accepted 2001 August 20; published 2001 September 5

### ABSTRACT

Recent observations of several  $\gamma$ -ray burst (GRB) afterglows have shown evidence for a large amount of X-ray line-emitting material, possibly arising from ionized iron. A significant detection of an X-ray spectral feature, such as that found in the *Chandra* observation of GRB 991216, may provide important constraints on the immediate environment of the burst and hence on progenitor models. The large Fe  $K\alpha$  equivalent widths inferred from the X-ray observations favor models in which the line is produced when the primary X-ray emission from the source strikes Thomson-thick material and Compton scatters into our line of sight. We present such reflection spectra here, computed in a fully self-consistent manner, and discuss the range of ionization parameters that may be relevant to different models of GRBs. We argue that the presence of a strong hydrogen-like  $K\alpha$  line is unlikely, because Fe xxvi photons would be trapped resonantly and removed from the line core by Compton scattering. In contrast, a strong narrow emission line from He-like Fe xxv is prominent in the model spectra. We briefly discuss how these constraints may affect the line energy determination in GRB 991216.

*Subject headings:* gamma rays: bursts — line: formation — radiation mechanisms: nonthermal

### 1. INTRODUCTION

The detection of spectral signatures associated with the environment of a  $\gamma$ -ray burst (GRB) would provide important clues about the triggering mechanism and the progenitor (Mészáros & Rees 1998; Lazzati, Campana, & Ghisellini 1999; Böttcher 2000). Observations with *Chandra*, *ASCA*, and *BeppoSAX* have provided tentative evidence for Fe  $K\alpha$  line and edge features in at least five bursts; GRB 970508 (Piro et al. 1999), GRB 970828 (Yoshida et al. 1999), GRB 991216 (Piro et al. 2000), and GRB 000214 (Antonelli et al. 2000) all show an emission feature during the X-ray afterglow a few hours to a day after the burst event, while GRB 990705 (Amati et al. 2000) displays a prominent X-ray absorption feature during the burst itself. Although most of the line detections are only marginally significant and fail to distinguish between the various line excitation mechanisms,<sup>1</sup> GRB 991216 shows a  $3.49 \pm 0.06$  keV line at a moderate confidence level ( $\sim 4\sigma$ ). This is consistent with emission from H-like Fe (Fe xxvi) at the redshift of the most distant absorption system along the line of sight at  $z = 1.02$  (Vreeswijk et al. 2000). A similar observation, but with a higher signal-to-noise ratio, may be able to distinguish between the various line emission mechanisms and lead to the correct determination of the line energy.

The large equivalent widths (EWs; approximately a few keV) inferred from the X-ray features favor models in which the line is produced by reflection (Vietri et al. 2001; Rees & Mészáros 2000) rather than transmission. Any detection of emission features in the afterglow spectra some hours after the burst (such as in GRB 991216) therefore imposes strong constraints on the location and geometry of the optically thick reflecting material. Observing an X-ray line at a time  $t_{\text{obs}}$  after the burst implies that the emitting material must be located within a distance  $\sim ct_{\text{obs}}/(1+z)$  from the explosion site, thus strongly limiting the size of the remnant. However, this gas cannot be optically thick along the line of sight because this would smear out the short time variability of the burst radiation. These conditions

point toward a strongly anisotropic environment from which a GRB is seen only if we happen to observe the system through a line of sight with low optical depth (Böttcher 2000; Vietri et al. 2001; Lazzati et al. 2001).

Two types of reflection models have been developed to explain the origin of the X-ray emission features. The first invokes the interaction of the primary X-ray emission from the afterglow with an Fe-enriched, Thomson-thick, asymmetric remnant, which Compton scatters X-rays into our line of sight (Vietri et al. 2001; Böttcher & Fryer 2001). This scenario requires a mass  $\geq 0.06 M_{\odot}$  of Fe at a distance about 1.5 lt-day, possibly due to a remnant of an explosive event or a supernova that occurred days or weeks prior to the GRB (see Vietri & Stella 1998; in contrast with MacFadyen & Woosley 1999, which favors a simultaneous supernova explosion). The other type of model involves a long-lived ( $\geq 1$  day) magnetar or accreting black hole with a continuing but decaying outflow that interacts with the stellar envelope at distances less than a light-hour (Rees & Mészáros 2000; Mészáros & Rees 2001). In this case, only a small mass of Fe is required and can be readily produced by the star itself.

Under both interpretations, it is likely that reflection takes place in highly ionized surfaces. This can lead to strong Comptonization of the emergent Fe line and other absorption and emission features. In this Letter, we present and discuss detailed, self-consistent computations of the temperature and ionization structure of a uniform slab of gas ionized by the incident radiation of a GRB and of the resulting reflection spectra. Our analysis applies to an optically thick, homogeneous medium, significantly extending previous analysis in the optically thin regime (e.g., Weth et al. 2000; Böttcher 2000), which is hard-pressed to explain the observed Fe-line feature in GRB 991216 (Vietri et al. 2001). We estimate the strength of the Fe  $K\alpha$  line that each model produces. Finally, we discuss the implications of these results for current and future X-ray observations.

### 2. X-RAY-ILLUMINATED SLABS

We employ the reflection code developed by Ross, Weaver, & McCray (1978) and updated by Ross & Fabian (1993). We consider the illumination of the first 12 Thomson depths of an

<sup>1</sup> The energy of the Fe emission line shifts up in energy from 6.4 through 6.7–6.97 keV as Fe is ionized, but Doppler shifts may confuse precise estimates of the observed energy.

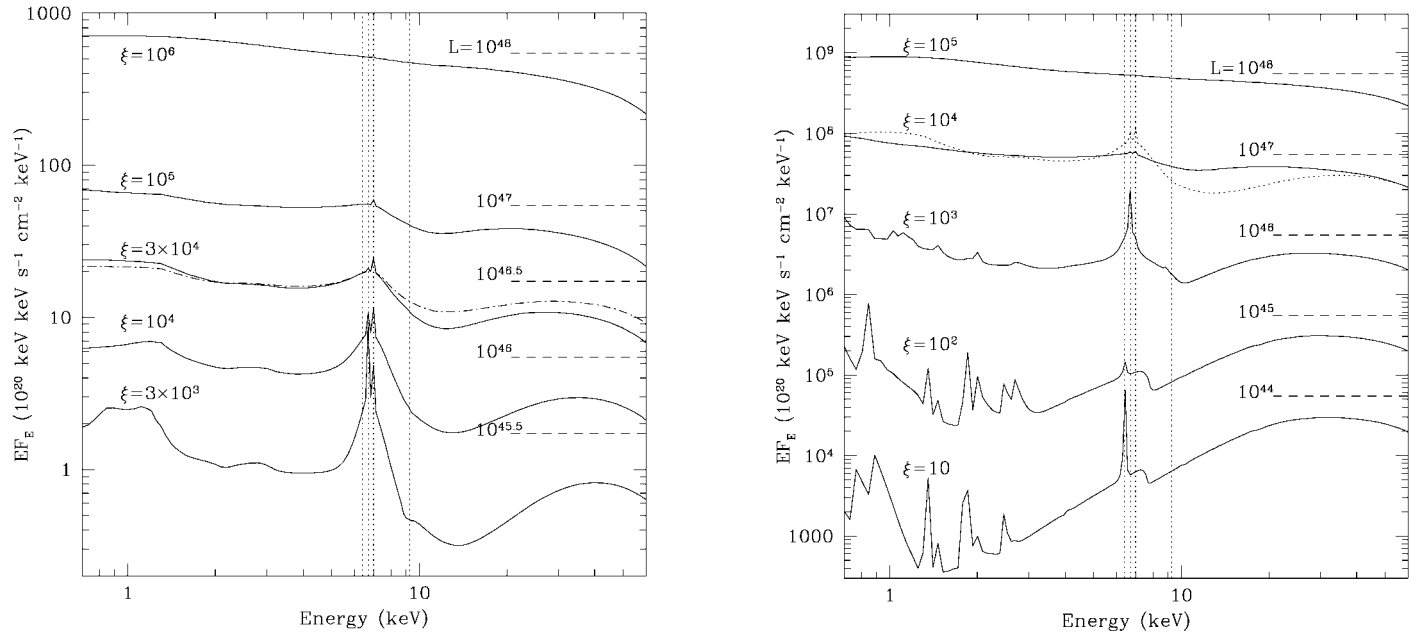


FIG. 1.—X-ray reflection spectra for illumination with a  $\Gamma = 2$  power law. In both panels, the vertical lines are at (from left to right) 6.4, 6.7, and 6.97 keV for the three different Fe  $K\alpha$  line energies and 9.28 keV, which is the energy of the iron recombination edge. *Left panel*: Illumination of a uniform supernova remnant with 10 times solar Fe abundance, various values of the afterglow luminosity, and  $\vartheta = 45^\circ$ . The ionization parameter is given by  $\xi_{\text{SN}} = 10^6 L_{48}$ , assuming  $d_{16} = 1$ ,  $n_{\text{H},10} = 1$  (see eq. [2]). From top to bottom, the EWs and the luminosities (integrated between 5.7 and 7.1 keV) inferred from the X-ray line features are 3, 37, 94, 268, and 943 eV and  $2.5L_{46}$ ,  $2.7L_{45}$ ,  $9.6L_{44}$ ,  $3.6L_{44}$ , and  $1.4L_{44}$ . The dot-dashed line illustrates the effect of increasing the incident angle from  $\vartheta = 45^\circ$  to  $\vartheta = 75^\circ$  at a constant luminosity. *Right panel*: Illumination of a funnel excavated in the stellar envelope with solar Fe abundance and various values of the decaying X-ray luminosity from the GRB central engine. In this case,  $\xi_{\text{SE}} = 10^5 L_{48}$ , assuming  $d_{13} = 1$ ,  $n_{\text{H},17} = 1$ ,  $\beta = 1$  (see eq. [3]) with  $\vartheta = 45^\circ$ . From top to bottom, the EWs and the luminosities inferred from the X-ray line features are 3 eV, 62 eV, 1.1 keV, 122 eV, and 1.6 keV and  $2.6L_{46}$ ,  $2.7L_{45}$ ,  $2.7L_{44}$ ,  $5L_{42}$ , and  $5.2L_{41}$ . The dotted line shows the reflected spectra for illumination with the same luminosity but into a stellar envelope that is 10 times more abundant in iron. The line luminosity and EW for this model are 243 eV and  $3.7L_{45}$ .

infinite, uniform slab of gas by radiation with a power-law spectrum of photon index  $\Gamma$  incident at an angle  $\vartheta$  to the normal (Ross, Fabian, & Young 1999). The incident radiation is treated analytically in a “one-stream” approximation, while the diffuse radiation that results from both the Compton scattering of the incident radiation and emission from the gas itself is treated using the Fokker-Planck/diffusion method of Ross et al. (1978). Once thermal and ionization equilibrium in the slab is found, the reflection spectrum is computed. We assume that hydrogen and helium are completely ionized but include the partially ionized species C v–vii, O v–ix, Mg ix–xiii, Si xi–xv, and Fe xvi–xxvii.

For a given  $\Gamma$ , the temperature and ionization state of the surface of the slab is expected to depend mainly on the value of the ionization parameter,

$$\xi = \frac{4\pi F}{n_{\text{H}}}, \quad (1)$$

where  $F$  is the total illuminating flux (from 0.01 to 100 keV) and  $n_{\text{H}}$  is the hydrogen number density (Ross et al. 1999).

### 3. APPLICATION TO GAMMA-RAY BURSTS

If the GRB explodes within a young supernova remnant, the X-rays from the afterglow will illuminate Fe-rich ( $\sim 10$  times solar Fe abundance) material, leading to recombination line emission by reflection (Vietri et al. 2001). Reasonable values of  $\xi$  expected in this scenario are

$$\xi_{\text{SN}} \approx 10^6 L_{48} d_{16}^{-2} n_{\text{H},10}^{-1}, \quad (2)$$

where  $L$  is the source luminosity in units of ergs per second,  $n_{\text{H}}$  is the hydrogen density in units of  $\text{cm}^{-3}$ , and  $d$  is the distance from the burst explosion to the material in units of centimeters. We adopt the convention  $Q = 10^x Q_x$  for expressing the physical parameters. The time delay of a few days observed in GRB 991216 yields an incident angle for the radiation of  $\vartheta \sim 45^\circ$  (Vietri et al. 2001).

Alternatively, line emission can be produced when a post-burst outflow, possibly magnetically dominated, impacts on the walls of a funnel excavated in the stellar envelope at distances less than a light-hour (Rees & Mészáros 2000). Luminosities as high as  $L \sim 10^{47}$  ergs  $\text{s}^{-1}$  are expected 1 day after the burst, if they are due either to the spinning down millisecond pulsar or to a highly magnetized torus around a black hole (Rees & Mészáros 2000). The ionization parameter in the stellar envelope case is

$$\xi_{\text{SE}} \approx \beta 10^4 L_{47} d_{13}^{-2} n_{\text{H},17}^{-1}, \quad (3)$$

where  $\beta < 1$  is the ratio of ionizing to MHD luminosity (Rees & Mészáros 2000). The incident flux would be deflected along the funnel walls with different incident angles before escaping the funnel: for simplicity we assume  $\vartheta \sim 45^\circ$ .

For these uniform-density slabs we vary  $\xi$  by changing the total illuminating flux while keeping the hydrogen number density  $n_{\text{H}}$ , the distance from the burst  $d$ , and the incident angle  $\vartheta$  fixed. Figure 1 shows the results for illumination by a  $\Gamma = 2$  spectrum for both of the scenarios described above. The illuminating and reflected spectra are displayed as  $EF_E$ , where  $F_E$  is the spectral energy flux and  $E$  is the photon energy. The models with the highest ionization parameter ( $\xi > 10^{4.5}$ ) are excellent reflectors and show almost no Fe spectral features.

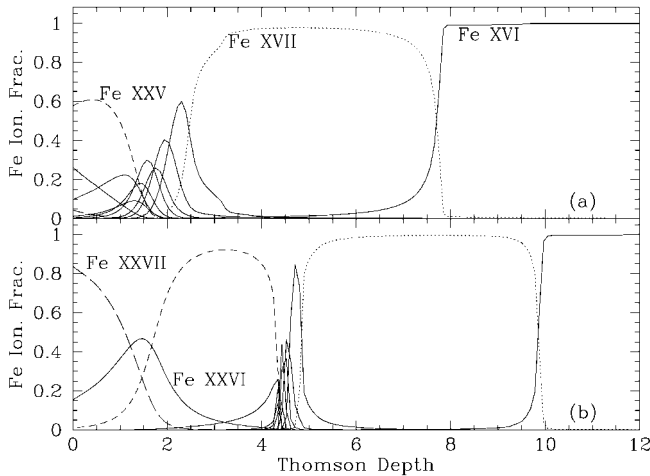


FIG. 2.—Fe ion fractions as a function of Thomson depth produced by the illumination of a uniform slab with  $\Gamma = 2$ . The same line type denotes the same species of Fe in both plots. (a) Illumination of a funnel excavated in the stellar envelope with solar Fe abundance and  $\xi_{SE} = 10^3$ . (b) Illumination of a uniform supernova remnant with 10 times solar Fe abundance and  $\xi_{SN} = 10^4$ .

This is because the surface layer is almost fully ionized, and Fe xxvi does not become dominant until  $\tau_T > 8$ . The temperature at the surface of the slab is  $\sim 1.9 \times 10^7$  K, the Compton temperature for the incident spectrum. The spectrum drops at  $\sim 50$  keV because we included a sharp energy cutoff in the incident spectrum at 100 keV.<sup>2</sup> Compton reflection produces a slight steepening in the reflected spectrum, which mimics a power law with  $\Gamma > 2$  in the 3–30 keV band. For example, we find  $\Gamma = 2.3$  in the  $L_{48}$  supernova case and  $\Gamma = 2.14$  in the  $L_{48}$  stellar envelope case.

When the illuminating flux is reduced so that  $10^{3.5} < \xi < 10^4$ , Fe K $\alpha$  emission and Fe K-shell absorption features begin to appear. Most of the K $\alpha$  photons originate at  $\tau_T \gg 1$  and emerge as broad Comptonized lines with weak cores. The H-like K $\alpha$  photons at 6.97 keV are generated close to the surface but are resonantly trapped and removed from the narrow-line core by Compton scattering. The He-like intercombination line at 6.7 keV is not subject to resonant trapping but is generated at such high  $\tau_T$  (see Fig. 2b) that it is multiply Compton scattered on leaving the slab. The broad Comptonized emission features blended into the Compton smeared K-shell absorption edge are an important signature of ionized reflection. The effect of increasing the iron abundance at a fixed ionization parameter is illustrated by the dotted line in Figure 1. The Comptonized line and the absorption feature are increasingly significant for an Fe-rich medium.

With  $\xi \sim 10^3$ , Fe xxv becomes dominant at  $\tau_T \approx 1$  (see Fig. 2a). A narrow emission line resulting from Fe xxv can now be seen superposed on the Compton-broadened emission bump. The tiny emission feature just above 8.8 keV results from radiative recombination directly to the ground level of Fe xxv (see the  $L_{46}$  stellar envelope case in Fig. 2). In the model with  $\xi_{SE} = 10^2$ , the Fe emission is suppressed because Fe xvii–xxii dominates close to the surface, but their K $\alpha$  photons are destroyed by the Auger effect during resonance trapping (Ross, Fabian, & Brandt 1996). Finally, for  $\xi_{SE} = 10$  the reflection spectrum is similar to that of a cold, neutral slab, and so the narrow emission line at 6.4 keV is dominant.

<sup>2</sup> For a constant-density slab and the values of  $\Gamma$  considered here, extending the illuminating spectrum to higher energies ( $< 511$  keV) would have little effect on the iron ionization and spectral features (e.g., Ross et al. 1999).

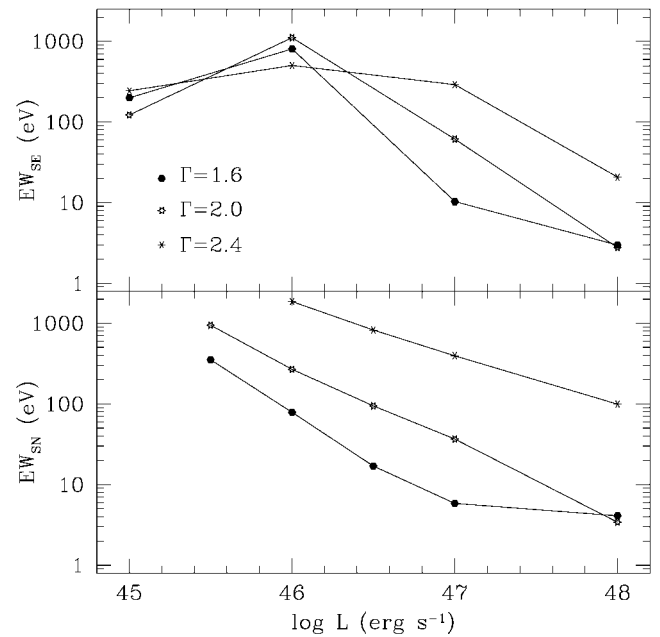


FIG. 3.—Fe K $\alpha$  EWs as a function of both the incident luminosity and  $\Gamma$  for the stellar envelope and supernova scenarios.  $\vartheta$  was taken to be  $45^\circ$  for these models. The EWs were computed from the calculated reflection spectra (integrated between 5.7 and 7.1 keV). If one uses the total spectrum (incident + reflected), then smaller EWs are obtained. For example, the EWs for  $\Gamma = 1.6$ , 2.0, and 2.4 when  $L = L_{46}$  (in both cases) are 370, 430, and 131 eV (stellar envelope) and 43, 145, and 805 eV (supernova).

The effect of increasing the incident angle  $\vartheta$ , which is a key ingredient in the preejection models because it is responsible for the observed time delay, is also illustrated in Figure 1 by the dot-dashed line. Radiation that illuminates the atmosphere more directly ionizes more deeply into the slab than radiation at grazing incidence. At high flux levels, the emergent line features are little changed; however, the K-shell absorption features become more prominent for radiation that impacts closer to the normal of the slab.

The ionization structure in the outer layers of the illuminated slab also depends on the incident radiation spectrum. Figure 3 shows the Fe K $\alpha$  EW as a function of incident luminosity for a series of reflection spectra with  $\Gamma = 1.6$ , 2.0, and 2.4, assuming  $\vartheta = 45^\circ$ . The EWs were calculated with respect to the reflection spectrum, and the integration was carried out between 5.7 and 7.1 keV. As seen in Figure 1, the EW of the Fe K $\alpha$  line decreases with  $L$  in both GRB scenarios. This behavior continues until  $L$  is sufficiently low for the narrow Fe K $\alpha$  emission line to be suppressed by the Auger effect. The EWs are generally larger when the illuminating spectrum is steeper (i.e.,  $\Gamma$  is greater). The weaker ionizing power of steep spectra allow line emission to persist at the highest luminosities, although the EWs still end up quite low when  $L = L_{48}$ . In a GRB, softer spectra may be important if both the line emission arises from the impact of the continuous energy output with the compact remnant and much of the observed continuum emission (with a flatter  $\Gamma$ ) comes from the afterglow emission directly.

#### 4. DISCUSSION

The emission feature observed  $\sim 1.5$  days after the GRB 991216 burst (Piro et al. 2000) had a line luminosity of  $L_{line} = 4 \times 10^{44}$  ergs  $s^{-1}$  and an EW of  $\sim 0.5$  keV. The continuum flux from GRB 991216, measured to have  $\Gamma =$

$2.2 \pm 0.2$ , in the 1–10 keV band was 50–100 times stronger than the flux in the line. As is clear from the above discussion, the emission feature can be explained by reflection if identified with the recombination  $K\alpha$  line from He-like iron at 6.7 keV.

Taking  $\Gamma \approx 2$  in the stellar envelope scenario, a continuous ionizing luminosity of  $\sim 10^{45}$ – $10^{46}$  ergs  $s^{-1}$  (or a continuous wind luminosity of  $10^{47}$  ergs  $s^{-1}$  with  $\beta \sim 0.01$ – $0.1$ ; see Rees & Mészáros 2000) would be sufficient to produce the observed line.<sup>3</sup> However, it is possible that the reflected and incident spectra are observed together. With the above parameters, the line luminosity and EW calculated for the total spectrum (reflected + incident) are  $L_{\text{line}} \sim 2 \times 10^{44}$  ergs  $s^{-1}$  and  $EW \sim 0.25$ – $0.7$  keV. If the illuminating spectrum is a steeper power law ( $\Gamma > 2$ ), then a smaller fraction of illuminating photons lie in the 9–20 keV range, which dominates the ionization of Fe, and thus an increase in either  $L$ ,  $\beta$ , or the Fe abundance is required in order to reproduce the same line strength (Fig. 3).

Alternatively, an X-ray afterglow with  $\Gamma \approx 2$  illuminating the walls of a supernova remnant with a luminosity of  $\sim 10^{45.5}$ – $10^{46}$  would produce a line signal with  $L_{\text{line}} \sim 2 \times 10^{44}$  ergs  $s^{-1}$  and  $EW \sim 0.2$ – $0.8$  keV. However, an essential assumption contained in this model is that the material responsible for emission-line features is illuminated by the early afterglow radiation (or the GRB itself) with  $L \geq L_{48}$ . Such high luminosities would cause the spectral features resulting from iron to disappear or, at best, to be extremely weak (even for larger values of  $\Gamma$ , see Fig. 3). Moreover, this early incident radiation can be harder than a  $\Gamma \sim 2$  spectrum with a significant fraction of the energy above the  $\gamma\gamma \rightarrow e^\pm$  formation energy threshold and a high compactness parameter. This will cause new pairs to be formed in the originally optically thick scattering medium, an effect that amplifies the density of scattering charges and increases the temperature of the illuminating material. When pairs are produced in sufficient numbers, the iron  $K\alpha$  emission is suppressed due to the decrease in the number of recombinations. These effects will be investigated elsewhere (D. Lazzati, E. Ramirez-Ruiz, & M. J. Rees 2001, in preparation). These problems may be overcome in particular source geometries for which lower luminosities and softer spectra are expected at the edges of the relativistic outflow.

The results presented in Figure 1 show that if the observed

<sup>3</sup> Under this interpretation, the observed line width can easily be reproduced by Comptonization for an expansion velocity below the limit of  $0.1c$  inferred by Piro et al. (2000).

Fe  $K\alpha$  line from GRB 991216 is identified solely with the H-like line at 6.97 keV, as suggested by Piro et al. (2000), then this is inconsistent with emission from a photoionized optically thick slab. Their detailed analysis of the *Chandra* Advanced CCD Imaging Spectrometer S chip spectrum shows marginal evidence (at the  $2.1 \sigma$  level) of an emission feature at  $4.4 \pm 0.5$  keV. Identifying this feature with the Fe recombination edge with rest energy of 9.28 keV gives  $z = 1.1 \pm 0.1$ , consistent with the redshift of an H-like Fe  $K\alpha$  line. Nonetheless, it is important to emphasize that the observations presented by Piro et al. (2000) do not rule out the presence of an He-like Fe feature (or a blend between H and He-like features as shown in Fig. 1). Some ambiguity also remains in the rest energy of the emission since Doppler blueshifts of order  $0.1c$  are expected in both reflection scenarios (Vietri et al. 2001; Rees & Mészáros 2000; Mészáros & Rees 2001) and may confuse precise measurements of the line energy. Indeed, for an expansion velocity of  $0.1c$ , the emission feature at  $4.4 \pm 0.5$  keV could be attributed to the Fe xxv radiative recombination emission just above 8.8 keV rather than to the Fe recombination edge at 9.28 keV.

Finally, Co produces both He and H-like emission lines: at 7.242 keV and just above 7.526 keV, respectively. The exact strength of these features, which we do not include in our calculations, could be important in both of the scenarios discussed here and may confuse the identification of low signal-to-noise ratio spectral features.

We have presented calculations of X-ray reflection from Thomson-thick slabs for conditions that may arise in the immediate environment of a GRB. Comparisons between putative Fe  $K\alpha$  lines detected in X-ray afterglows and those predicted by the computations will be useful in distinguishing between the various line emission mechanisms. We expect that more sensitive data on X-ray afterglow spectral features will impose strong constraints on the nature of GRB progenitors and their environments.

We thank M. J. Rees, P. Mészáros, D. Lazzati, A. Blain, and the referee for useful comments and suggestions. We are particularly grateful to A. C. Fabian and R. R. Ross for very helpful insights regarding the calculations. E. R.-R. acknowledges support from CONACYT, SEP, and the ORS foundation. D. R. B. thanks the Commonwealth Scholarship and Fellowship Plan and the Natural Sciences and Engineering Research Council of Canada for support.

## REFERENCES

- Amati, L., et al. 2000, *Science*, 290, 953  
 Antonelli, A., et al. 2000, *ApJ*, 545, L39  
 Böttcher, M. 2000, *ApJ*, 539, 102  
 Böttcher, M., & Fryer, C. L. 2001, *ApJ*, 547, 338  
 Lazzati, D., Campana, S., & Ghisellini, G. 1999, *MNRAS*, 304, L31  
 Lazzati, D., Ghisellini, G., Amati, L., Frontera, F., Vietri, M., & Stella, L. 2001, *ApJ*, 556, 471  
 MacFadyen, A. I., & Woosley, S. E. 1999, *ApJ*, 524, 262  
 Mészáros, P., & Rees, M. J. 1998, *MNRAS*, 299, L10  
 ———. 2001, *ApJ*, 556, L37  
 Piro, L., et al. 1999, *ApJ*, 514, L73  
 ———. 2000, *Science*, 290, 955  
 Rees, M. J., & Mészáros, P. 2000, *ApJ*, 545, L73  
 Ross, R. R., & Fabian, A. C. 1993, *MNRAS*, 261, 74  
 Ross, R. R., Fabian, A. C., & Brandt, W. N. 1996, *MNRAS*, 278, 1082  
 Ross, R. R., Fabian, A. C., & Young, A. J. 1999, *MNRAS*, 306, 461  
 Ross, R. R., Weaver, R., & McCray, R. 1978, *ApJ*, 219, 292  
 Vietri, M., Ghisellini, G., Lazzati, D., Fiore, F., & Stella, L. 2001, *ApJ*, 550, L43  
 Vietri, M., & Stella, L. 1998, *ApJ*, 507, L45  
 Vreeswijk, P. M., et al. 2000, *GCN Circ.* 496 (<http://gcn.gsfc.nasa.gov/gcn3/gcn3/496.gcn3>)  
 Weth, C., Mészáros, P., Kallman, T., & Rees, M. J. 2000, *ApJ*, 534, 581  
 Yoshida, A., et al. 1999, *A&AS*, 138, 433